Direct Current Cathodic Glow Discharge Polymerization of Methane and Butane

MASAYO MIYAMA, HIROTSUGU K. YASUDA

Center for Surface Science and Plasma Technology, and Department of Chemical Engineering, University of Missouri–Columbia, Columbia, Missouri 65211, USA

Received 25 July 1997; accepted 6 February 1998

ABSTRACT: The deposition of a polymeric material on the surface of the cathode of a direct current (dc) glow discharge was investigated for methane and butane. The cathode region of a dc glow discharge is not a plasma in a strict sense. Consequently, the deposition of a polymeric material to the cathode surface differs significantly from so-called plasma polymerization of the same monomer (starting gas or vapor) that deposits on a substrate placed in a glow discharge plasma. Using methane and *n*-butane, the influence of the molecular weight of the monomer (M), volume flow rate, and discharge power on the deposition rate in a dc glow discharge were investigated and compared with those in an audio frequency and a radio frequency glow discharge. It was found that the deposition rate expressed in (thickness growth rate)/(M) is linearly proportional to the current density, which implies that cathodic polymerization is controlled by the cathode region parameter (not plasma parameters). The refractive indices (632.8 nm) for the cathodic polymers are in the range of 2.2–2.4 while those for plasma polymers are in the range of 1.5–1.7. © 1998 John Wiley & Sons, Inc. J Appl Polym Sci 70: 237–245, 1998

Key words: direct current cathodic glow discharge; methane; butane; polymerization

INTRODUCTION

When organic molecules, such as methane or butane, are allowed to interact with a glow discharge plasma or a glow discharge plasma of such a gas is created, the formation of a thin film deposition of polymeric material is observed. When such a process is carried out at ambient temperature (without heating the substrate on which the deposition occurs), it is often called "plasma polymerization" or "glow discharge polymerization."[1–4] Such a process is distinguished from chemical vapor deposition (CVD) because the activation of molecules occurs strictly in the plasma phase.[5]

When a direct current (dc) glow discharge is used for plasma polymerization, the deposition occurs nearly exclusively on the cathode surface; a plasma polymerization results in deposition on every surface exposed to a plasma and also on surfaces in the downstream, including the reactor wall. This is an extremely favorable feature for the surface modification of conducting substrates, because the deposition occurs only on the substrate (used as the cathode) and eliminates contamination of the reactor. This advantageous feature of dc glow discharge has not been exploited in the past, and the major portion of research on plasma polymerization has been devoted to radio frequency (RF) glow discharges. It has been recently demonstrated that dc cathodic polymerization can be effectively utilized in corrosion protection of cold rolled steel.[6–10]

From the viewpoint of mechanistic aspects of material deposition, it is important to recognize

Correspondence to: H. K. Yasuda.

Contract grant sponsor: National Science Foundation; contract grant number: CTS-9400725.

Journal of Applied Polymer Science, Vol. 70, 237–245 (1998)

 CCC 0021-8995/98/020237-09

that the cathode region of a dc glow discharge is not a plasma in a strict sense because a disparity exists in the density of positive charge and that of negative charge. The cathode surface is continuously bombarded with accelerated ions; consequently, material growth occurs under the bombardment of ions. Therefore, it is anticipated that the dependence of deposition on operational parameters, as well as the characteristics of the deposited film, should be significantly different from those for plasma polymers of the same monomer. We present experimental data pertinent to these questions.

EXPERIMENTAL

Materials

Methane (99.0% min.) and *n*-butane (99.5% min.) gases were purchased from Matheson Gas Products, Inc., and used without further purification. As substrates, pieces of silicon wafers (2 × 2 cm) were used after being ultrasonically cleaned in acetone.

An unpolished low carbon automotive grade cold rolled steel panel (Advanced Coating Technologies Laboratories, Inc.) was used as a cathode in full size (10.2 × 15.2 × 0.08 cm) or quarter size (5.1 × 7.6 × 0.08 cm) after cleaning thoroughly with acetone for the dc glow discharge polymerization.

Polymerization

The dc cathodic polymerization and audio frequency (AF) and RF plasma polymerization were carried out in bell jar type reactors. A schematic representation of the reactors is shown in Figure 1. The inside diameter of the glass bell jars were 43.5 and 44.5 cm, and the total volumes of the reactor chambers were approximately 75 and 80 L.

The first reactor was used for a dc cathodic polymerization. The dc power was supplied by a MDX-1K magnetron drive (Advanced Energy Industries, Inc.) and controlled by current. Two stainless steel plates (25.4 × 25.4 × 0.16 cm) were used as anodes, and they were grounded. The separation was fixed at 15.2 cm. In the anode magnetron discharge, eight permanent magnet bars were evenly attached on the back of each of the anodes in a circular configuration and the south poles were oriented toward the center.

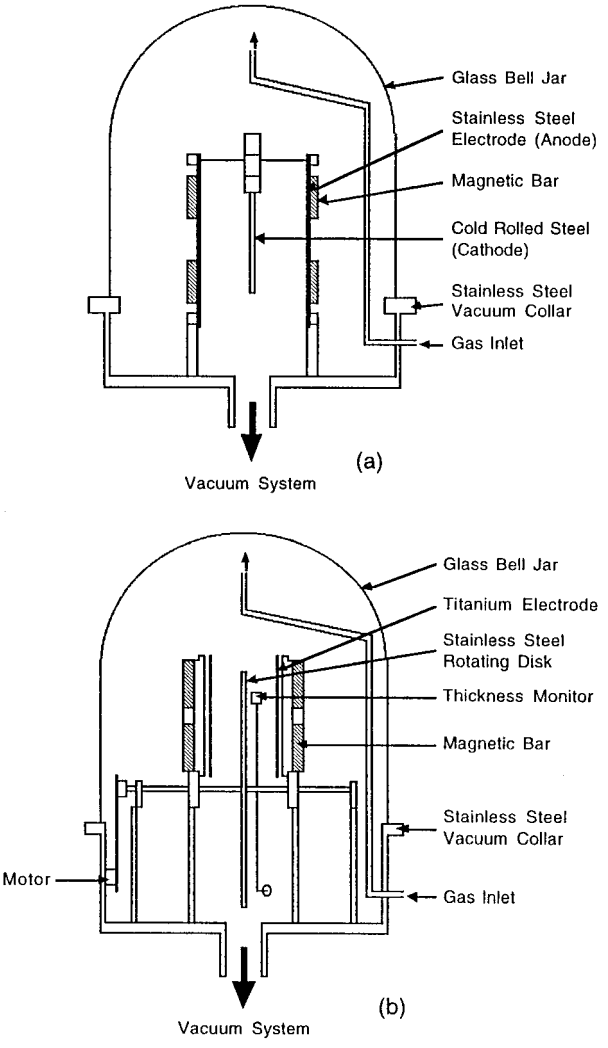

Figure 1 Schematic representation of (a) dc cathodic polymerization reactor and (b) AF and RF plasma polymerization reactor.

A cold rolled steel panel was used as a cathode placed midway between the two parallel anodes. Substrates were mounted on the cold rolled steel plate (cathode) and silver print was used to provide a conducting path between the substrate and the cathode. Before the polymerization, the cathode was treated with a glow discharge of an argon and hydrogen gas mixture as a final cleaning step to prevent it from sparking; the polymerization was carried out without exposure to air.

The current density was calculated from the current measured by a multimeter (3435A, Digital Multimeter, Hewlett–Packard) divided by total cathode area.

AF and RF plasma polymerizations were carried out in another reactor [Fig. 1(b)] which was a Shimadzu plasma polymerization apparatus

Table I Types of Polymerization

	Type	Magnets	Magnet Position	Substrate Position
1	Anode magnetron dc cathodic polymerization	Yes	On anodes	On cathode
2	dc cathodic polymerization	No	—	On cathode
3	AF plasma polymerization	Yes	On electrodes	Midway between electrodes
4	RF plasma polymerization	Yes	On electrodes	Midway between electrodes
5[a]	Anode magnetron dc cathodic polymerization	Yes	On anodes	Midway between electrodes
6[a]	AF plasma polymerization	No	—	On electrode
7[a]	RF plasma polymerization	No	—	On electrode

[a] Carried out for comparison.

(LCVD-1200-400A). Glow discharge was created at 15 kHz (AF) by using an internal power source AF-400 (Kyoto Denkiki Co., Ltd.) or at 13.56 MHz (RF) by using an external RFX-600 generator and ATX-600 tuner (Advanced Energy Industries, Inc.). The AF power was controlled by current, and the RF power was controlled by wattage.

Six permanent magnet bars were evenly arranged on the back side of each of the titanium electrodes (17.8 × 17.8 × 0.16 cm) in a circular configuration with the south poles oriented toward the center. The electrode separation was fixed at 8.5 cm. Substrates were mounted on a stainless steel rotating disk (35.6-cm diameter) placed midway between the electrodes. The radial positions of the substrates were 14 cm from the center of the disk. For uniform deposition, the disk was rotated at a speed of 15 rpm during the process. The substrates were located in the interspace between the electrodes for 20–25% of the rotation.

In both reactors the bell jar chambers were evacuated by two pumps in series, one rotary pump and one mechanical booster pump. After the pressure in the reactor reached its minimum attainable value (less than 4 mtorr), the gas was fed in through a tube with its outlet located above the interelectrode space facing the bell jar wall. The pressure was measured with a MKS Baratron pressure transducer. The flow rate, F, in standard cubic centimeters per minute (sccm) of each gas was controlled with an MKS or Tylan mass flow controller and determined by using the ideal gas equation in conjunction with measurement of $\Delta p/\Delta t$ taken with the pump valve off. The mass flow rate is given by $FM \times (4.46 \times 10^{-5})$ in grams per minute, where M is the molecular weight of the gas. The system pressure of the reactor was controlled by a throttle valve coupled with the pressure meter at 6.7 Pa (50 mtorr).

The polymerization types that were carried out in this study are summarized in Table I.

Measurement of Thickness and Refractive Index

An AutoEL-II automatic ellipsometer (Rudolph Research Corporation), which is a null-seeking type with a 632.8-nm helium-neon laser light source, was used for measurement of the thickness and refractive index of deposited films. Deposited films with approximately 50-nm thickness were prepared. The thickness growth rates of the deposited films were simply calculated from thickness divided by glow discharge time. In the AF and RF plasma polymerizations, about half of the deposition occurred outside of the interspace between the electrodes.

RESULTS AND DISCUSSION

Deposition Rates

Local deposition parameters (at a specific place on the substrate) are as follows: k_1 is the mass deposition rate (kg/m^2 s); k_2 is the thickness growth rate (m/s); $k_2 = k_1/\rho$, where ρ is the specific gravity (kg/m^3); k_0 is the specific mass deposition rate (1/m^2); and $k_0 = k_1/FM$ is the mass flow rate corrected deposition rate.

Mass Balance

Consider the following parameters *per unit time:* the total mass of the monomer introduced into the system is $W_1 = FM$, the total mass of the deposition is W_2, the monomer–polymer conversion ratio is $Y_p = W_2/W_1$ (polymerization yield of a monomer), and total surface area is S.

$$W_2 = \oint_s k_1 ds$$

$$S = \oint ds$$

$$k_0 = \frac{k_1}{W_1} = \frac{k_1}{FM}$$

$$\bar{k}_0 = \frac{W_2}{S \cdot FM} = \frac{\bar{k}_1}{FM}$$

$$\bar{k}_1 = \frac{\oint_s k_1 ds}{\oint ds}$$

where $\bar{k}_1$ is the average deposition rate and $\bar{k}_0$ is the average specific deposition rate. The total mass of gaseous effluent, W_3, is

$$W_1 = W_2 + W_3$$

Plasma polymerization generally requires the production of gaseous nonpolymerizable by-products in order to create new chemical bonds for polymerization. For instance, plasma polymerization of saturated hydrocarbons requires hydrogen abstraction by plasma state gas. In the presence of double and triple bonds, the hydrogen production becomes very small.

Polymer yield ($Y_p = W_2/W_1$) cannot be unity because of the gas formation for which the gas yield can be defined by $Y_g = W_3/W_1$. The value of Y_p and Y_g can be determined by measurement of the pressure of a closed system that is subjected to the plasma state. If this Y_p can be considered as a physicochemical parameter characteristic to a specific monomer, the average specific deposition rate can be expressed by

$$\bar{k}_0 = Y_p W_1 \left(\frac{1}{S}\right)$$

where the first term Y_p is the monomer characteristic; the second term, the mass flow rate, is an operational parameter; and the third term $(1/S)$ is a factor of reactor design. In other words, the average specific deposition rate or the average deposition rate obtained by plasma polymerization is a function of the monomer, operational parameter, and the design factor of the reactor employed.

deposition rate = F(monomer characteristics, operational parameter, design factor)

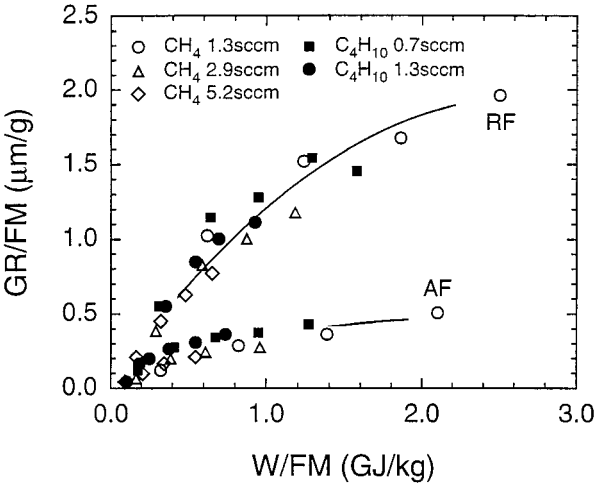

Figure 2 Dependence of GR/FM on W/FM for AF and RF plasma polymerizations. The flow rates for methane were 1.3, 2.9, and 5.2 sccm and for n-butane were 0.7 and 1.3 sccm.

The deposition rate generally reported in the literature is the local deposition rate k_1, and the thickness growth rate generally used is the local thickness growth rate k_2. In cathodic polymerization, S is nearly equal to the electrode surface area, which provides a unique situation to deal with "deposition rate." In the less well-defined plasma polymerization, however, it has been well established that the deposition rate and properties of plasma polymers primarily depend on the value of W/FM in joules/kilogram, which is the energy per unit mass of gas or vapor to create plasma.[2] When dealing with various monomers having different molecular weights, deposition rate (DR) or thickness growth rate (GR) can be normalized by dividing the value by the mass flow rate FM.

Figure 2 illustrates how well the thickness growth rate, GR/FM, in AF and RF plasma polymerizations of methane and n-butane can be expressed as a function of the input parameter W/FM. It is important to recognize that, regardless of the mass of the monomer and flow rate, a single line fits all data obtained in AF or RF plasma polymerizations in which the deposition occurs on an electrically floating conductor or on a dielectric substrate.

When we applied the same principle to express the thickness growth rate in dc cathodic polymerization, it became quite clear that the cathodic polymerization is not an ordinary plasma polymerization. Figure 3 depicts the same kind of plots as those shown in Figure 2. There is a clear

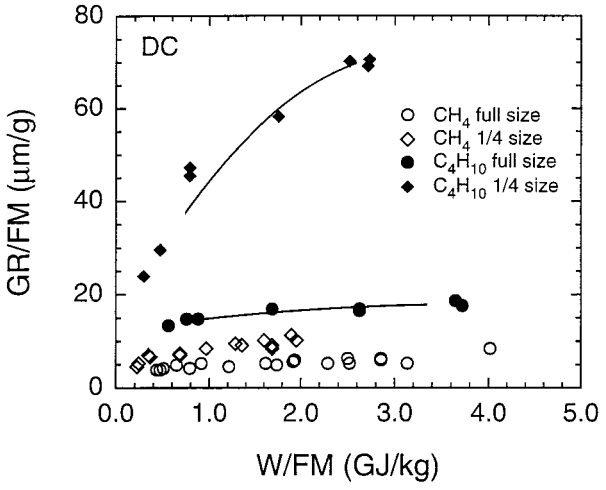

Figure 3 Dependence of GR/*FM* on *W*/*FM* for dc cathodic polymerization. The cathode size was full and $\frac{1}{4}$, flow rate for methane was 2.8 sccm and for *n*-butane was 0.8 sccm.

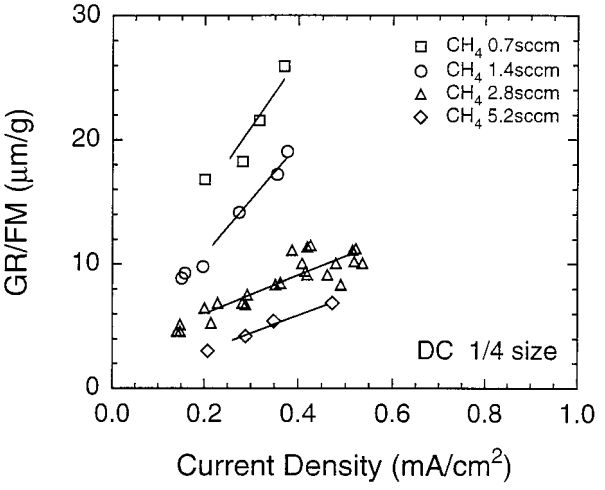

Figure 5 Dependence of GR/*FM* on current density for dc cathodic polymerization of methane at cathode size $\frac{1}{4}$. The flow rates were 0.7, 1.4, 2.8, and 5.2 sccm.

dependence on *W*/*FM*, but no normalized curve can be obtained. There is a clear difference due to the size of the substrate (cathode) and the mass of the monomer. In simple terms, the general trend found for plasma polymerization does not apply to cathodic polymerization.

If we plot the same data against the current density of the discharge, the data for methane converge to a single line and that for *n*-butane converge to another line as shown in Figure 4. It should be noted that data shown in Figure 3 and Figure 4 were obtained at a fixed flow rate for each monomer. When various flow rates are employed, the plots show different lines depending on flow rate, as shown in Figure 5 for methane.

The best universal dependency was found between GR/*M* and current density. Figure 6 depicts this relationship for all dc cathodic polymerization data obtained in this study covering experimental parameters such as flow rate, size of cathode, mass of monomer, and the presence or absence of magnetic enhancement on the anode.

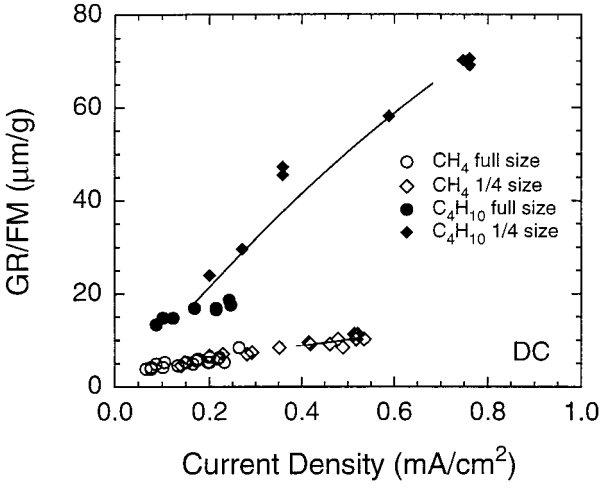

Figure 4 Dependence of GR/*FM* on current density for dc cathodic polymerization. The cathode size was full and $\frac{1}{4}$, flow rate for methane was 2.8 sccm and for *n*-butane was 0.8 sccm.

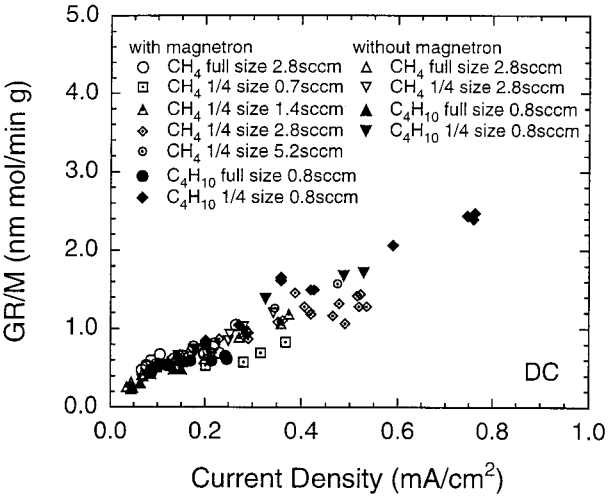

Figure 6 Dependence of GR/*M* on current density for dc cathodic polymerization. The cathode size was full, flow rate for methane was 2.8 sccm and for *n*-butane was 0.8 sccm with magnetron discharge; cathode size was $\frac{1}{4}$, flow rates for methane were 0.7, 1.4, 2.8, and 5.2 sccm and for *n*-butane was 0.8 sccm without magnetron discharge.

Table II Influence of Flow Rate on Thickness Growth Rate for dc Cathodic Polymerization of Methane

Flow Rate (sccm)	Current (mA)	Voltage (V)	Wattage (W)	Current Density (mA/cm^2)	W/FM (GJ/kg)	Growth Rate (nm/min)	GR/FM (mm/g)	GR/M (nm mol/min g)
0.7	15	1107	17	0.20	1.18	8.4	16.7	0.53
1.4	15	1054	16	0.20	0.57	9.8	9.8	0.61
2.8	16	997	16	0.22	0.28	11.0	5.3	0.69
5.2	15	965	14	0.21	0.14	11.3	3.1	0.71
0.7	26	1579	41	0.37	3.69	13.1	25.9	0.82
1.4	26	1437	37	0.36	1.69	17.0	17.1	1.06
2.8	26	1386	36	0.36	0.80	17.5	8.4	1.09
5.2	26	1254	33	0.35	0.40	20.0	5.4	1.25

Cathode size, $\frac{1}{4}$.

The details of the experimental data for film growth rates are summarized in Table II and Table III.

Table II provides a summary of the influence of flow rate on the thickness growth rates for dc cathodic polymerization of methane. At higher flow rates, less voltage is required to maintain a given current. Higher flow rates also lead to slightly higher growth rates but lower values of GR/FM.

Table III is a summary of the magnetron discharge effects for dc cathodic polymerization of methane. As shown, higher voltages are required to achieve a given current without magnets. Anode magnetron discharge increases the ionization probability. This higher ionization probability leads to a lowering of the breakdown voltage and increases the capability for applying high energies. Without an anode magnetron, a negative glow was observed in most of the interelectrode space. In contrast, a funnel-shaped negative glow was observed when a magnetron was used as an anode.[11]

The implication of the correlation shown in Figure 6 is that the cathode region of a dc glow discharge is indeed not a plasma, and the energy input parameter (to plasma phase) does not control the deposition of material onto the cathode surface. The current density of a dc glow discharge is the prime operational parameter. It also shows that the flow rate of monomer does not influence the film thickness growth rate. The film thickness growth rate is dependent on the mass of monomer rather than the mass input rate (FM), which is the determining factor in plasma polymerization.

These observations indicate that dc cathodic polymerization is controlled by the events occurring in the cathode region only. It appears that the fragmentation of monomer in the gas phase is

Table III Effect of Anode Magnetron on Cathodic Polymerization of Methane

Cathode Size	Magnets (mA)	Current	Voltage (V)	Wattage (W)	Current Density (mA/cm^2)	W/FM (GJ/kg)	Growth Rate (nm/min)	GR/FM (μm/g)	GR/M (nm mol/min g)
Full	Yes	20	735	15	0.067	0.43	7.6	3.7	0.47
Full	Yes	40	1075	43	0.133	1.22	9.8	4.6	0.61
Full	No	20	1145	23	0.067	0.66	6.8	3.2	0.42
Full	No	41	1721	70	0.133	2.08	9.3	4.6	0.58
$\frac{1}{4}$	Yes	10	780	8	0.141	0.23	9.5	4.6	0.59
$\frac{1}{4}$	Yes	20	1157	24	0.283	0.68	14.5	6.9	0.91
$\frac{1}{4}$	No	10	1181	12	0.143	0.34	10.3	4.9	0.64
$\frac{1}{4}$	No	20	1662	34	0.280	0.97	15.4	7.3	0.96

Flow rate, 2.8 sccm.

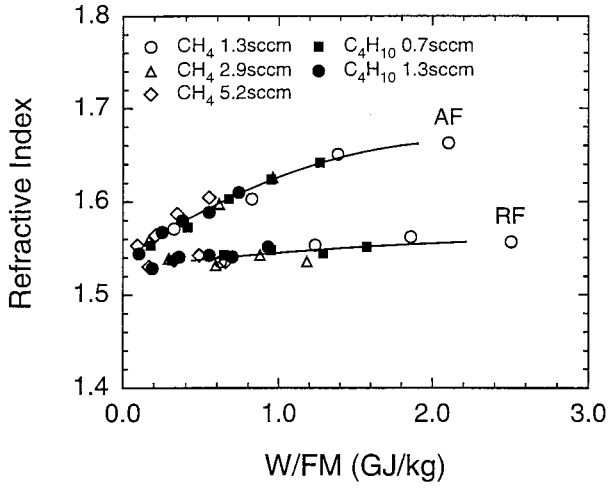

Figure 7 Relationship between *W/FM* and refractive index of deposited films for AF and RF plasma polymerizations. The flow rates for methane were 1.3, 2.9, and 5.2 sccm and for *n*-butane were 0.7 and 1.3 sccm.

minimal, which leads to the direct proportionality of film thickness growth rate on the mass of the monomer. It also suggests that the cathode region of a dc glow discharge is a separate entity in which the concentration of monomer is controlled by the current density and is not controlled by the mass flow rate in the reactor.

Refractive Index

Figure 7 shows the relationship between *W/FM* and the refractive indices of films grown from methane and *n*-butane by AF and RF plasma polymerizations. For each mode, all data points lie on a single curve that is independent of flow rate and monomer molecular weight. For AF plasma polymerization, the refractive index is higher than for RF plasma polymerization, and the increase in refractive index with an increase in *W/FM* is more significant.

Figure 8 shows refractive index versus *W/FM* for films grown by dc cathodic polymerization of methane and *n*-butane monomers for two cathode sizes with and without use of magnetron discharge. The data from Figure 7 are shown for comparison. The refractive index values for films grown by dc cathodic polymerization are significantly higher than those grown by AF and RF plasma polymerizations and are similar in value to those of diamond (2.42). There is no significant variation of refractive index with changes in *W/FM* or current density.

The refractive index of these films can be related to properties such as compactness and hardness, because a higher refractive index implies a higher density of materials in the film. Scratch tests were carried out to investigate these properties. The films deposited by dc cathodic polymerization were very hard, and none could be scratched by a small screw driver. In contrast, all samples synthesized by AF and RF plasma polymerizations could be scratched. It is expected that ion bombardment is much stronger for dc cathodic polymerization than for AF and RF plasma polymerizations. It has been reported that lower system pressure[12] and higher substrate temperature[13] give higher values of the refractive index to plasma polymerized films; the film shows a higher density, lower hydrogen content, and more inorganic structure. These facts suggest that more hydrogen atoms are abstracted from monomer molecules and more inorganic structure film deposits for the dc cathodic polymerization.

Difference between Substrate on Electrode and Floating Substrate

In comparing glow discharge polymerization of a monomer prepared by different power sources (e.g., from dc to RF), it is necessary to consider the

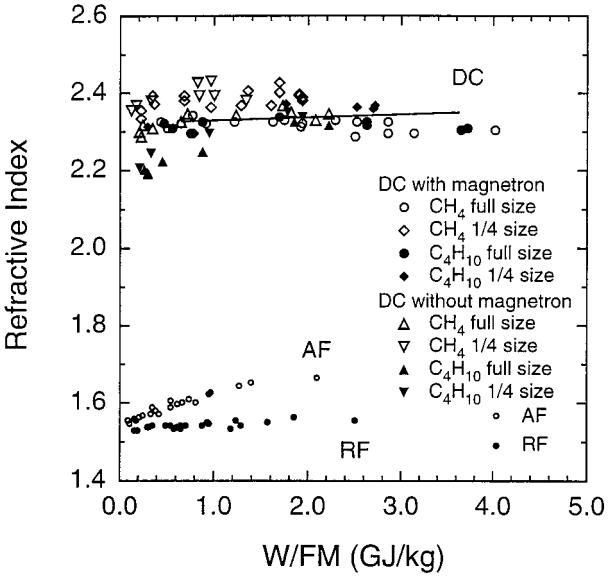

Figure 8 Comparison of refractive index of deposited films for dc cathodic polymerization and AF and RF plasma polymerizations as a function of *W/FM*. DC: the cathode size was full and $\frac{1}{4}$, flow rate for methane was 2.8 sccm and for *n*-butane was 0.8 sccm. AF and RF: the flow rates for methane were 1.3, 2.9, and 5.2 sccm and for *n*-butane were 0.7 and 1.3 sccm.

Table IV Characteristics of Plasma Polymers of Methane Deposited Under Various Conditions

	Frequency	Magnets	Conductivity[a]	W/FM (GJ/kg)	Current Density (mA/cm^2)	Growth Rate (nm/min)	Refractive Index	Scratch
On electrode	dc[b]	No	Yes	0.21	0.034	4.0	2.30	No
	dc[c]	Yes	Yes	1.90	0.523	23.0	2.40	No
	dc[c]	Yes	No	1.22	0.393	5.8	2.08	Yes
	AF	No	Yes	1.21	0.063	1.7	2.19	No
	AF	No	No	1.21	0.064	1.4	2.19	No
	RF	No	Yes	1.25	—	1.4	1.56	Yes
Floating	dc[c]	Yes	—	1.24	0.372	5.7	1.75	Yes
	AF	Yes	—	2.18	0.126	0.5	1.67	Yes
	RF	Yes	—	2.50	—	1.9	1.55	Yes

Flow rates: dc, 2.8 sccm; AF, 1.3 sccm; RF, 1.3 sccm.
[a] Electrical connection to an electrode; the cathode was used in dc discharge.
[b] Cathode size, full.
[c] Cathode size, $\frac{1}{4}$.

location of a substrate on which a plasma polymer deposits. The most obvious difference in dc cathodic polymerization and other glow discharges is that the substrate in the cathodic polymerization is the cathode; but in the AF and RF modes used in this study, a substrate is placed in the plasma phase (not on an electrode). This difference can be seen as a floating substrate versus a substrate placed on an electrode.

In order to investigate the effect of the modes of the substrate, experiments involving types 5, 6, and 7 (Table I) were added. Table IV summarizes the growth parameters and corresponding film properties for a number of films grown on floating and nonfloating substrates by either dc cathodic polymerization or AF or RF plasma polymerization. Without exception, all films deposited on floating substrates have a lower refractive index. An RF plasma polymerization film had a low refractive index, regardless of the position of a substrate.

These results can best be understood on the basis of the degree of ion bombardment during film growth. Ion bombardment at a film surface is much more intense when located on an electrode than when it is floating. Ion bombardment is also stronger at lower frequencies. When ion bombardment is strong, the deposited films lose their polymeric structure due to the abrasion of hydrogen atoms. The films become more amorphous carbon structures with a high refractive index. The refractive index of the film is in the order $dc_{electrode} > dc_{floating}$, $AF_{electrode} > AF_{floating}$, $RF_{electrode} = RF_{floating}$.

CONCLUSIONS

The dc cathodic polymerization of methane or *n*-butane is an entirely different process from plasma polymerization of the same monomer. In cathodic polymerization, the deposition of film is controlled by the parameters of the cathode region, which is not a plasma in a strict sense. The deposition of film in the ordinary mode of plasma polymerization is controlled by the parameters of the plasma. The film thickness growth rate in the cathodic polymerization is a function of current density and mass of monomer. This is a clear deviation from plasma polymerization in which the film thickness growth rate is a function of the energy input rate to plasma (energy per unit mass of monomer in unit time) and mass flow rate.

The characteristics for films deposited by dc cathodic polymerization are different from those deposited by AF or RF plasma polymerization. Films deposited by cathodic polymerization have a very high refractive index and hardness, similar to those for a hard amorphous carbon structure.

The AF glow discharge polymer that deposits on an electrode, regardless of electrical connection, has similar characteristics to the dc cathodic polymer (electrode effect). In the RF glow discharge no electrode effect was found. The extent of ion bombardment during the process of plasma polymerization/deposition seems to be responsible for the electrode effect.

The use of a magnetron in the anode lowers the discharge voltage at a fixed current and, according to our recent studies, yields smoother distribution of deposition on a substrate; however, no

discernible difference was found in the current density dependence of the thickness growth rate and in the characteristics of deposited films.

REFERENCES

1. J. H. Hollahan and A. T. Bell, Eds., *Techniques and Applications of Plasma Chemistry,* Wiley, New York, 1974.
2. H. Yasuda, *Plasma Polymerization,* Academic, Orlando, FL, 1985.
3. R. d'Agostino, Ed., *Plasma Deposition, Treatment, and Etching of Polymers,* Academic, San Diego, CA, 1990.
4. H. Biederman and Y. Osada, *Plasma Polymerization Processes,* Elsevier Science, Amsterdam, 1992.
5. H. Yasuda, in *New Methods of Polymer Synthesis,* Vol. 2, J. R. Ebdon and G. C. Eastmond, Eds., Blackie Academic & Professional, Chapman & Hall, Glasgow, U.K., 1995, p. 161.
6. T. J. Lin, B. H. Chun, H. K. Yasuda, D. J. Yang, and J. A. Antonelli, *J. Adhes. Sci. Technol.,* **5,** 893 (1991).
7. W. J. van Ooij, D. Surman, and H. K. Yasuda, *Prog. Org. Coat.,* **25,** 319 (1995).
8. H. Yasuda, B. H. Chun, D. L. Cho, T. J. Lin, D. J. Yang, and J. A. Antonelli, *Corrosion,* **52,** 169 (1996).
9. T. F. Wang, T. J. Lin, D. J. Yang, J. A. Antonelli, and H. K. Yasuda, *Prog. Org. Coat.,* **28,** 291 (1996).
10. H. K. Yasuda, T. F. Wang, D. L. Cho, T. J. Lin, and J. A. Antonelli, *Prog. Org. Coat.,* **30,** 31 (1997).
11. W. H. Tao, M. A. Prelas, and H. K. Yasuda, *J. Vac. Sci. Technol. A,* **14,** 2113 (1996).
12. R. Szeto and D. W. Hess, *J. Appl. Phys.,* **52,** 903 (1981).
13. M. R. Wertheimer, J. E. Klemberg–Sapieha, and R. Corriveau, *Can. J. Phys.,* **60,** 628 (1982).